



A Numerical Analysis of the Performance of Linear Interpolation Schemes Coupled with Finite Volume Method in determining Velocity Distribution for Confined Convection-Diffusion Turbulent Flow Field.

Jane Gatwiri¹, Stephen Karanja¹, David Theuri²

¹Meru University of Science and Technology, Meru, Kenya.

²Jomo Kenyatta University of Agriculture and Technology, Kenya.

ARTICLE INFO

ABSTRACT

KEY WORDS

Turbulent flow

Interpolation

Discretization

convection, diffusion

Numerical methods are widely used to obtain solutions of fluid flow problems because they well compliment experimental methods. The numerical results obtained are however never exact due to errors emanating from the scheme used in discretizing the governing equations and the flow domain. For convection-diffusion flow, the magnitudes of these errors vary depending on the scheme used to interpolate the nodal values of the flow quantities to the interfaces. The precision level of an interpolation scheme is determined by its ability to minimize these errors hence generating results that are consistent with experimental results. This paper documents the performance of three linear interpolation schemes; upwind differencing, central differencing scheme and the hybrid scheme in obtaining velocity profiles for a convection-diffusion turbulent flow field. The field variables present in the governing equations are decomposed into a mean and a fluctuating component and averaged so as to reduce the enormous scales inherent in a turbulent flow regime. The closure problem was solved using the turbulence model. The turbulence equations have been converted into discrete form using the robust finite volume discretization technique. The discretized equations are solved using a segregated pressure-based algorithm. The numerical results were validated using the benchmark results of Ampofo and Karayiannis, (2003). The results revealed that linear interpolation schemes are not appropriate in analyzing velocity distribution for confined convection-diffusion turbulent flows because the results obtained using all the three linear schemes were inconsistent with experimental results.

* Corresponding author: Jane gatwiri. Email: janemuteagatwiri@gmail.com

<https://doi.org/10.58506/ajstss.v1i2.125>

AFRICAN JOURNAL OF SCIENCE, TECHNOLOGY AND SOCIAL SCIENCES ISSN :2958-0560

<https://journals.must.ac.ke> © 2022 The Authors. Published by Meru University of Science and Technology

This is article is published on an open access license as under the CC BY SA 4.0 license

Background of the study

In fluid dynamics, flow behavior is analyzed experimentally, analytically or numerically. Though experimental methods are capable of producing physically realistic results, they are expensive, and less flexible. Analytical solutions of most flows occurring in practical applications are either unavailable, or computationally inefficient. Solutions of most flows are thus obtained numerically. However, the results are never exact due to discretization errors inherent in numerical methods. In the Finite volume discretization method, the solution domain is subdivided into cells referred to as finite volumes. The transported variable is stored at the center of the finite volume. Since the flow is continuous, the flux entering a given volume is identical to the flux leaving the adjacent volume then, the method is conservative. The finite volume discretization method is geometrically flexible and can therefore be used for any type of geometry. The method uses integral formulation of conservation laws which makes it superior to other numerical methods because in differential form, one makes the assumption that the solution is continuous. The major challenge of the finite volume method is obtaining the interface values of flow variables in a convection-diffusion flow field. Various schemes that interpolate the centered values of the flow quantities to the interfaces are found in literature. Each of these schemes is anchored on a certain assumption about the distribution of the flow quantity from the center of a finite volume to the interfaces. This paper documents the performance of three linear interpolation schemes in analyzing velocity profiles for a convection-diffusion turbulent flow in a cavity.

Review of Previous Related Studies

Various interpolation schemes have over the years been used to interpolate nodal values of flow variables. A numerical analysis of temperature and velocity distribution in a cubic enclosure locally heated from below was carried

out by (2) in 2003. The equations governing the flow were discretized using the Finite Difference approximation method. The Central Differencing scheme was used to obtain interphase values of the dependent variables. Results revealed unstable thermal stratification within the enclosure.

In 2013, a comparative study of three numerical turbulence models ($k-\varepsilon$, $k-\omega$ and $k-\omega-SST$) in predicting heat transfer due to natural convection inside an air filled differentially heated cavity, was carried out by (1). The flow regime was considered turbulent. The Finite Difference Approximation method coupled with the Hybrid differencing scheme was used. The results showed that the $k-\omega-SST$ model performed better than the $k-\varepsilon$ and the $k-\omega$ turbulence models in the whole enclosure.

A numerical analysis of steady natural convection phenomena of air in a square cavity heated from the bottom was carried out by (5) in 2015. The governing equations along with the boundary conditions were discretized using the Finite Difference Method coupled with the central difference interpolation scheme. Results showed that increase in temperature difference between the vertical walls affects the fluid dynamic behavior by increasing the intensity of flow in the enclosure. Conduction was found to dominate low Rayleigh number flows while convection was found to be dominant for higher Rayleigh number flows.

In 2017, a parametric study of turbulent natural convection in an enclosure with localized heating and cooling was carried out by (4). The Finite Volume method coupled with the Power Law interpolation scheme was used. The results revealed that the velocity decreases with distance from the walls, increases with increase in Rayleigh number, and decreases with increase in aspect ratio.

In 2017, natural convection of air in a square cavity with partially thermally active side walls was studied by (3) The behavior of boundary layers at variable Rayleigh numbers was

analyzed. The Finite Volume Method was used to discretize the governing equations. The Central Differencing interpolation scheme was used to

Governing Equations

The fluid flow is governed by the general conservation laws of mass, momentum and energy.

Mass Conservation Equation

$$\frac{\partial \rho}{\partial t} + \frac{\partial}{\partial x_j} (\rho u_j) = 0 \quad (1)$$

Momentum Conservation Equation

$$\frac{\partial}{\partial t} (\rho u_i) + \frac{\partial}{\partial x_j} (\rho u_i u_j) = -\frac{\partial P}{\partial x_i} + \rho g_i + \frac{\partial}{\partial x_j} \left[\mu \left(\frac{\partial u_i}{\partial x_j} + \frac{\partial u_j}{\partial x_i} \right) + \mu_s \delta_{ij} \frac{\partial u_k}{\partial x_k} \right] \quad (2)$$

Energy Conservation Equation

$$\rho \left[\frac{\partial}{\partial t} (C_p T) + \frac{\partial}{\partial x_j} (C_p u_j T) \right] = \frac{\partial}{\partial x_j} \left(\lambda \frac{\partial T}{\partial x_j} \right) + \beta T \left(\frac{\partial p}{\partial t} + \frac{\partial u_j p}{\partial x_j} \right) + \Phi \quad (3)$$

In a turbulent flow field, each of the flow variables is regarded as consisting of a mean or average value ($\bar{\phi}$) and a fluctuating value (ϕ') such that:

$$\phi(x, t) = \phi'(x, t) + \bar{\phi}(t) \quad (4)$$

ϕ Denotes the value of a flow property at a particular instance and location, whereas $\bar{\phi}$ and ϕ' denotes the mean and fluctuating values of ϕ respectively. This technique of separating the average and the fluctuating parts of a quantity is referred to as Reynolds decomposition. The average value $\bar{\phi}$ is defined as

$$\bar{\phi} = \frac{1}{\Delta t} \int_{t_0}^{t_0 + \Delta t} \phi(x, t) dt \quad (5)$$

where Δt is the time averaging interval chosen such that it is sufficiently large. This implies that the mean value $\bar{\phi}$ is a function of space only.

Consequently,

$$\bar{\phi}(x, t) = \bar{\phi}(x_i) \quad (6)$$

obtain interface values. Results showed that for $10^3 \leq Ra \leq 10^6$, the flow regime was laminar.

The governing equations 1-3 are decomposed and averaged, and assumptions coupled with the Boussinesq assumption imposed to yield

$$\frac{\partial \bar{U}_j}{\partial x_j} = 0 \quad (7)$$

$$\frac{\partial U_i}{\partial t} + U_j \frac{\partial U_i}{\partial x_j} = -\frac{1}{\rho} \frac{\partial P}{\partial x_i} + \frac{\partial}{\partial x_j} \left[\nu \frac{\partial U_i}{\partial x_j} - \overline{u_i u_j} \right] + [1 - \beta(T - T_0)] g_i \quad (8)$$

$$\frac{\partial T}{\partial t} + U_j \frac{\partial T}{\partial x_j} = \alpha \frac{\partial^2 T}{\partial x_j^2} - \frac{\partial}{\partial x_j} (\overline{u_j T}) \quad (9)$$

Treatment of Turbulent Correlations

In equations (8) and (9), the correlations $\overline{u_i u_j}$ and $\overline{u_j T}$ are unknown. These terms emanate from the fluctuation motion. In addition to the stresses caused by pressure and viscosity effects, a fluid element experiences stresses emanating from the turbulent fluctuations. These correlations account for the additional momentum and energy transport in turbulent flow. The presence of these turbulent correlations in the Reynolds averaged equations therefore creates need for closure. Researchers have over the years attempted to resolve the closure problem. Among the numerous attempts is turbulence modeling, an approach that either expresses the turbulent correlations in terms of known quantities or through direct resolution of the correlations. In turbulence modeling, the $k - \epsilon$ equation is the most fundamental since it describes the budget of turbulent kinetic energy. The equation is given as

$$\left\{ \begin{aligned} & \frac{\partial}{\partial t} (\overline{\rho k}) + \frac{\partial}{\partial x_j} (\overline{\rho u_j k}) = - \frac{\partial}{\partial x_j} \left(\underbrace{\frac{1}{2} \overline{\rho u_i' u_i' u_j'}}_{\text{iii}} + \underbrace{\overline{p' u_j'}}_{\text{iv}} - \underbrace{\mu \frac{\partial k}{\partial x_j}}_{\text{v}} \right) - \underbrace{\overline{\rho u_i' u_j'}}_{\text{vi}} \frac{\partial u_i}{\partial x_j} \\ & + \underbrace{\beta g \overline{\rho u_i' T'}}_{\text{vii}} - \underbrace{\mu \frac{\partial u_i'}{\partial x_j} \frac{\partial u_i'}{\partial x_j}}_{\text{viii}} \end{aligned} \right\} \quad (10)$$

The turbulent dissipation ε in the $k - \varepsilon$ model represents the rate of dissipation of turbulent kinetic energy. The ε - equation is derived from the Navier- Stokes equation for fluctuation vorticity.

Modeling the Unknown Correlations in the $k - \varepsilon$ Equation

The kinetic energy equation (10) has most of its terms containing unknown correlations emanating from velocity fluctuations in the turbulent flow. It is therefore necessary that we model these correlations by use of similarity considerations together with the Boussinesq assumptions. The modeled kinetic energy equation is given as

$$\frac{\partial k}{\partial t} + U_j \frac{\partial k}{\partial x_j} = \nu_t \left[\frac{\partial u_i}{\partial x_j} + \frac{\partial u_j}{\partial x_i} \right] \frac{\partial u_i}{\partial x_j} + \frac{\partial}{\partial x_j} \left[(\nu \sigma_k + \nu_t) \frac{\partial k}{\partial x_j} \right] + \beta g \frac{\nu_t}{\sigma_k} \frac{\partial T}{\partial x_i} - \varepsilon \quad (11)$$

where ε is the dissipation rate of turbulent kinetic energy.

In order to obtain the $k - \varepsilon$ turbulence model, we need an equation for ε . According to (8),

$$\varepsilon = c_\mu k \omega \quad (12)$$

Substituting equation (12) into equation (11) yield

$$\left\{ \begin{aligned} & \frac{\partial k}{\partial t} + U_j \frac{\partial k}{\partial x_j} = \nu_t \left[\frac{\partial u_i}{\partial x_j} + \frac{\partial u_j}{\partial x_i} \right] \frac{\partial u_i}{\partial x_j} + \frac{\partial}{\partial x_j} \left[(\nu \sigma_k + \nu_t) \frac{\partial k}{\partial x_j} \right] \\ & + \beta g \frac{\nu_t}{\sigma_k} \frac{\partial T}{\partial x_i} - c_\mu k \omega \end{aligned} \right\} \quad (13)$$

The Shear-Stress Transport $k - \omega$ Turbulence Model

The $k - \varepsilon$ turbulence model is preferred in explaining flow behavior in the free stream region of a flow domain, while the $k - \omega$ model best accounts for flow behavior near a solid boundary. Mentor (1994), developed the *SST* $k - \omega$ turbulence model by putting into consideration the strengths and weaknesses of the $k - \varepsilon$ and the $k - \omega$ turbulence models. This model makes use of the $k - \omega$ model near the solid boundary, and transforms to the $k - \varepsilon$ model in the free stream region. For this reason, the *SST* $K - \omega$ turbulence model is considered in the current study because it well accounts for the flow behavior in the entire flow domain.

The turbulence equations for the *SST* $k - \omega$ are represented as follows:

$$\frac{\partial k}{\partial t} + U_j \frac{\partial k}{\partial x_j} = \frac{\partial}{\partial x_j} \left(\Gamma_k \frac{\partial k}{\partial x_j} \right) + P_k + G_k - Y_k \quad (14)$$

$$\frac{\partial \omega}{\partial t} + U_j \frac{\partial \omega}{\partial x_j} = \frac{\partial}{\partial x_j} \left(\Gamma_\omega \frac{\partial \omega}{\partial x_j} \right) + P_\omega + D\omega - Y_\omega \quad (15)$$

The modeled turbulent kinetic energy equation is represented by equation (14). Using a similar

approach, we now model equation (15) as follows:

$$\left\{ \begin{array}{l} \Gamma_\omega = (\nu + \sigma_\omega \nu_t), P_\omega = \gamma P_k, Y_\omega = \beta^* \omega^2, \\ D_\omega = 2\sigma\omega_2(1-F_1) \frac{1}{\omega} \frac{\partial k}{\partial x_j} \frac{\partial \omega}{\partial x_j} \end{array} \right\} \quad (16)$$

Substituting equation (16) into equation (15) yield:

$$\left\{ \begin{array}{l} \frac{\partial \omega}{\partial t} + U_j \frac{\partial \omega}{\partial x_j} = \frac{\partial}{\partial x_j} \left[(\nu + \sigma_\omega \nu_t) \frac{\partial \omega}{\partial x_j} \right] + \gamma P_k + \\ 2\sigma\omega_2(1-F_1) \frac{1}{\omega} \frac{\partial k}{\partial x_j} \frac{\partial \omega}{\partial x_j} - \beta^* \omega^2 \end{array} \right\} \quad (17)$$

Equations (8), (9),(10) (14) and (17) give the final set of model equations.

Table 1 Model Constants for the SST $k - \omega$ Turbulence Model.

$\sigma_{k,1}$	$\sigma_{k,2}$	$\sigma_{\omega,1}$	$\sigma_{\omega,2}$	α_*	c_μ	$\beta_{i,1}$	$\beta_{i,2}$	β^*_∞	β_i	Re_ω
0.85	1	0.5	0.857	0.31	0.09	0.075	0.0828	0.09	0.072	2.95

The set of equations governing the flow contain more variables than the number of equations. In fluid dynamics, the use of a suitable non-dimensional scheme is of paramount importance in reducing the number of parameters. In addition, Non dimensionalization enables both experimental and analytical results to be expressed in the most efficient form and makes the solution bounded. Besides, it enables us to obtain results of a flow regime experiencing a given set of conditions by making use of the results of a geometrically similar flow. In this regard, choose U to represent characteristic velocity, L_R to represent the characteristic length and ΔT_* to represent the characteristic temperature. All other physical properties will be non-dimensionalized using their respective values at a reference temperature T_0 . We now apply the relevant scaling variables to the final set

of modeled equations to obtain the non-dimensional form of the turbulent equations as follows:

$$\frac{\partial U'_j}{\partial X'_j} = 0 \quad (18)$$

$$\left[\frac{\partial U'_i}{\partial t'} + U'_j \frac{\partial U'_i}{\partial X'_j} = -\frac{1}{\rho'} \frac{\partial P'}{\partial X'_i} + \frac{\partial}{\partial X'_j} \left[\nu' \sqrt{\frac{\text{Pr}}{\text{Ra}}} \frac{\partial U'_i}{\partial X'_j} - \overline{u'_i u'_j} \right] + [1 - \beta' \beta_0 (\partial \theta \nabla T_*)] g'_i g_R \right] \quad (19)$$

$$\frac{\partial \theta}{\partial t'} + \frac{\partial \theta}{\partial X'_j} [U'_j - \overline{u'_j}] = \frac{\alpha'}{\sqrt{\text{Ra Pr}}} \frac{\partial}{\partial X'_j} \left[\frac{\partial \theta}{\partial X'_j} \right] \quad (20)$$

$$\left\{ \begin{array}{l} \frac{\partial k'}{\partial t'} + U'_j \frac{\partial k'}{\partial X'_j} = \frac{\nu'_i \nu_0}{L_R} \left[\frac{\partial U'_i}{\partial X'_j} + \frac{\partial U'_j}{\partial X'_i} \right] \frac{\partial U'_i}{\partial X'_j} + \frac{\text{Pr}}{\text{Ra}} \frac{\partial}{\partial X'_j} \left\{ (\nu' + \nu'_i \sigma_k) \frac{\partial k}{\partial X'_j} \right\} \\ + \frac{\beta' \beta_0 g'_i g_0 \nu'_i \nu_0 \Delta T_* L_R^2}{\alpha_0^2 \text{Ra Pr}} - \frac{\alpha_0}{L_R} C_\mu k' \omega' \sqrt{\text{Ra Pr}} \end{array} \right\} \quad (21)$$

$$\left\{ \begin{array}{l} \frac{\partial \omega'}{\partial t'} + U'_j \frac{\partial \omega'}{\partial X'_j} + \frac{\text{Pr}}{\text{Ra}} \frac{\partial}{\partial X'_j} \left[(\nu' + \sigma_\omega \nu'_i) \frac{\partial \omega'}{\partial X'_j} \right] + \frac{L_R}{\alpha_0 \sqrt{\text{Ra Pr}}} \left[\frac{\partial U'_i}{\partial X'_j} + \frac{\partial U'_j}{\partial X'_i} \right] \frac{\partial U'_i}{\partial X'_j} \\ - \frac{\alpha_0 \sqrt{\text{Ra Pr}} \beta^* \omega'^2 + 2\sigma\omega_2 [1-F_1]}{L_R} \frac{1}{\alpha_0 \sqrt{\text{Ra Pr}}} \frac{1}{\omega'} \frac{\partial k'}{\partial X'_j} \frac{\partial \omega'}{\partial X'_j} \end{array} \right\} \quad (22)$$

3.1 Velocity Boundary Conditions

Since the walls of the cavity are considered solid and impermeable, it means that motion can only be possible in its own plane, and hence, the normal components of velocity are zero. This is because mass cannot penetrate an impermeable solid surface. Therefore the velocity components $u = v = 0$. The velocity boundary conditions are thus stated as follows:

$$\left\{ \begin{array}{l} u(x=0, y) = v(x=0, y) = 0 \\ u(x=L_x, y) = v(x=L_x, y) = 0 \\ u(x, y=0) = v(x, y=0) = 0 \\ u(x, y=L_y) = v(x, y=L_y) = 0 \end{array} \right\} \quad (23)$$

Numerical Method

The transport equations presented in section 3.0 can be expressed into a generic conservation form that comprises of all the processes that influence the change of a dependent variable in a finite volume. The generic conservation form of the transport equations is given as

$$\frac{\partial \phi}{\partial t} + \frac{\partial}{\partial x_j} (u_j \phi) = \frac{\partial}{\partial x_j} \left(\Gamma \phi \frac{\partial \phi}{\partial x_j} \right) + S\phi \quad (24)$$

Where ϕ, Γ_ϕ and $S\phi$ are the dependent variable, exchange coefficient and source term of ϕ respectively. The generic conservation equation has four distinct terms which define the processes that affect the transport of ϕ in a finite volume. These are the temporal term, the convection term, the diffusion term and the source term. According to (7), the integral form of the generic conservation equation is given as.

$$\int_{VP} \frac{\partial \phi}{\partial t} dv + \frac{\partial}{\partial x_j} \int_{VP} (u_j \phi) dv = \frac{\partial}{\partial x_j} \int_{VP} \left(\Gamma_\phi \frac{\partial \phi}{\partial x_j} \right) dv + \int_{VP} S\phi dv. \quad (25)$$

Both the convection and the diffusion terms of equation (26) represent the flux of ϕ across the faces of a finite volume.

The discretized form of the generic conservation equation is given in summation form as

$$\phi_{ij} = \frac{\sum a_{nb} \phi_{nb} + b_{ij}}{a_{ij}} \quad (26)$$

In equation (26), the coefficient a_{nb} represents the contribution of each of the neighboring finite volumes to the dependent variable ϕ_{ij} , whereas a_{ij} contains the contribution of all terms influencing ϕ_{ij} . The coefficient b contains the contribution of the source terms. We obtain a discretization equation of the form of equation (26) for temperature in each finite volume. We adopt an iterative segregated algorithm to solve the equations. The relation below is used to

modify the values of the coefficients obtained in each iteration.

$$\phi_{ij} = \sigma \phi_{ij}^{predicted} + (1 - \sigma) \phi_{ij}^o \quad (27)$$

the relaxation factor is $\sigma \leq 1$.

In equation (27), $\phi_{ij}^{predicted}$ is the value of the new iteration whereas ϕ_{ij}^o is the value of the solution variable in the previous iteration.

Convergence Criterion

Once the values ϕ_{ij} have been obtained for temperature in all the finite volumes, the solution is modified using equation (27). We now obtain the absolute residual measure of the dependent variable using the relation below:

$$R_{ij} = \left| a_{ij} \phi_{ij} - \sum_{nb} a_{nb} \phi_{nb} - b \right| \quad (28)$$

However, since the values of coefficients a_{nb} and b changes in each finite volume, it is necessary that we obtain the local relative error by scaling the local residual relative to local value of the quantity such that

$$R_{ij}^{scaled} = \frac{\left| a_{ij} \phi_{ij} - \sum_{nb} a_{nb} \phi_{nb} - b \right|}{a_{ij} \phi_{ij}} \quad (29)$$

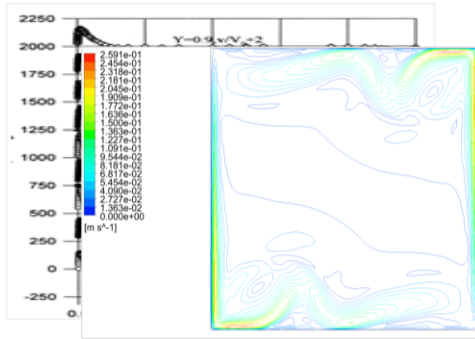
In the entire computational domain, we thus obtain the overall measure of the scaled residual as

$$R^\phi = \frac{\sum_{ALL\ CELLS} \left| a\phi - \sum_{nb} a_{nb} \phi_{nb} - b \right|}{\sum_{ALL\ CELLS} |a\phi|} \quad (30)$$

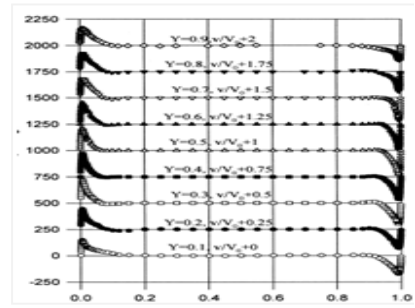
Equation (30) is used to monitor the convergence of an equation. If the overall residual reduces by three orders of magnitude then, the solution is said to be approaching the actual solution. Once the conservation equations have converged, the solution does not change with further iteration. Consequently, the conservation equations are satisfied in the entire solution domain.

The schemes are presented.

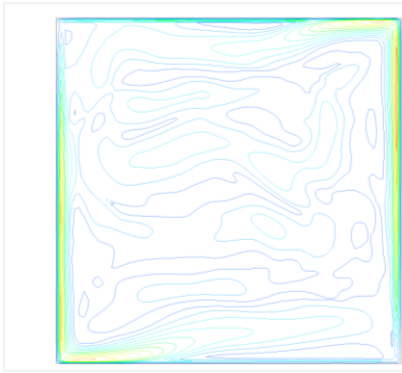
Results and Discussion



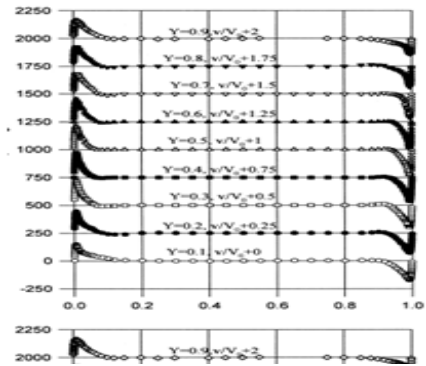
Hybrid Scheme



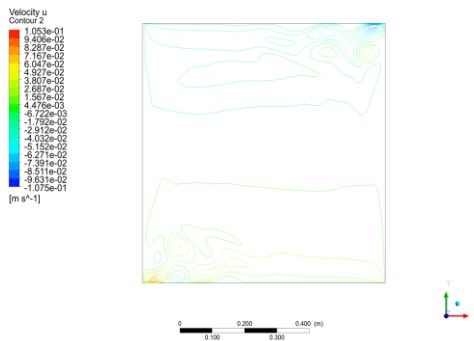
Benchmark Results



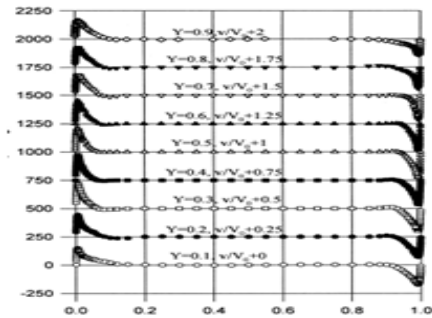
Upwind Difference



Benchmark Results



Central Difference Scheme



Benchmark Results

The results obtained reveal a non-uniform velocity distribution within the flow domain with some regions having higher velocities. For all the three sets of results, velocity is generally high at the upper right and bottom left regions of the flow domain. The central part of the flow domain is virtually stagnant. There are high velocity gradients along the vertical wall of the cavity indicating heat transfer by convection. The magnitude of velocity decreases with increase in distance from the walls of the cavity. However, the numerical results obtained using all the three linear interpolation schemes were inconsistent with bench mark results.

Conclusion.

Based on the above findings, we conclude that linear interpolation schemes are not appropriate for analyzing velocity distribution for convection-diffusion turbulent flows in confined settings.

Recommendations for Further Study

In order to gain more acumen on interpolation schemes, we recommend further research in the following areas:

- (i). Analyzing the distribution of other flow variables like pressure and turbulence in confined settings.
- (ii). Extension of the study to include non-linear interpolation schemes in analyzing velocity profiles.
- (iii). Extension of the study to include multiple heat sources in the flow domain.

References

Ampofo, F., & Karayiannis, T. G. (2003). Experimental benchmark data for turbulent natural convection in an air filled square cavity. *International Journal of Heat and Mass Transfer*, 46(19), 3551-3572.

Awuor, K. O. (2013). *Simulating Natural Turbulent Convection Fluid Flow in an Enclosure theTwo-Equation Turbulent Models* (Doctoral dissertation, Doctoral dissertation).

de Vahl Davis, G. (1986). Finite difference methods for natural and mixed convection in enclosures. *Proceedings in the 8th International Heat Transfer Conference*, vol. 1, 101-109. San Francisco, USA.

Kane, M., Cheikh, M., Lamine, S and Joseph, S. “ Natural Convection of Air in a Square Cavity with Partially Thermally Active Side Walls”. *Open Journal of Fluid Dynamics*, vol. 7, no.4

Karanja, S., Sigey, J., Gatheri, F., & Kirima, E. (2017). Turbulent Natural Convection in an Enclosure at Varying Rayleigh Number. *International Journal of Sciences: Basic and Applied Research*. 34 (2).

Noor-A-Alam Siddiki (2015). “Free Convection Heat Transfer in a Square Cavity heated from below and symmetrically cooling from the sides.” *International Journal of innovative Science Engineering and Technology*, vol 2, no.8

Versteeg, H., & Malalasekera, W. (2007). *An Introduction to Computational Fluid Dynamics: The Finite Volume Method*. Pearson Education Limited.

Wilcox, D. C. (1988). Multiscale model for turbulent flows. *AIAA journal*, 26(11), 1311-1320.